Electronic Supplementary Information

Application of Reduced Graphene Oxide for Hole Transport Layer in Organic Solar Cells Synthesized from Waste Dry Cell Using Electrochemical Exfoliation Method

Asfaw Negash[1]*, Aknachew M. Demeku[2], Liboro Hundito Molloro[1,3]

[a]College of Natural and computational Sciences, Department of Chemistry, Debre Berhan University, POBOX 445, Debre Berhan, Ethiopia

[b]College of Natural and computational Sciences, Department of Material Science and Engineering, Debre Berhan University, POBOX 445, Debre Berhan, Ethiopia

[c]State Key Laboratory of Silicate Materials for Architectures, Wuhan University of Technology (WUT), No. 122, Luoshi Road, Wuhan 430070, P. R. China

*Corresponding author: asfawdbu@gmail.com or AsfawNegash@dbu.edu.et

Contents

1. Experimental section

1.1. Instrumentation

The photoactive materials $PC_{71}BM$ 99% purity (Solenne b.v,), ITIC) (Solarmer Energy Inc., USA), IEICO-4F (1-MATERIAL INC), and PTB7-Th (Solenne b.v,) were purchased. The chemical structures of the photo-active materi- als are depicted below. Tetrabutyl ammonium hexafluorophosphate (Sigma- Aldrich, 99% purity) and anhydrous acetonitrile (Sigma-Aldrich) was used as the supporting electrolyte for the electrochemical investigations.

Poly(3,4- ethylenedioxythiophene):poly (styrene sulfonate) (PEDOT:PSS) (Heraeus, Cle- vios P VP.AI 4083) was used as interlayers in the device stacks. Chlorobenzene (CB) used as host solvents, and 1-chloronaphthalene (CN) as solvent additives. Both host solvent and solvent additives were obtained from Sigma-Aldrich. Aluminum (Al), used as the low work function cathode for the conventional devices. Indium doped tin oxide (ITO) (100 nm, Kintec, sheet resistivity 20 Ω sq^{-1}) was used as the transparent bottom electrode. Graphite rod is collected from waste dry cell batteries and used as raw material for the synthesis of GO and rGO. H_2O_2 (30%, Merck), hydrazine hydrate (90-100%, RENKEM), and NaOH (98%, Merck) were used for this study.

1.2. Characterization Techniques

1.2.1. UV-Vis-NIR Spectrometer

UV-Vis-NIR spectrophotometer measurements were conducted to measure absorbance spectra measurements and performed on a Perkin Elmer Lambda 950 spectrophotometer. The optical gap (Eg^{opt}) values of films of the conjugated polymers were calculated from the absorption onset wavelength ($\lambda onset$).

$$E_g = \frac{1240}{\lambda_{onset}} eV \quad \text{.....S1}$$

1.2.2. Conductivity Measurements

The conductivity was performed using the digital conductivity meter (Model 4510 Conductivity/TDS Meter). The powder graphite (G), graphene oxide (G), and reduced graphene oxide (rGO) dispersed in deionized water with a concentration variation from 0.004-0.01 ppm. The digital conductivity meter was adjusted by potassium chloride (Kcl) solution near 1.395 ms/cm with a cell constant 0.99. Its unit is typically expressed in micro Siemens/cm (μS/cm).

1.2.3. Cyclic Voltammetry

Cyclic voltammetry (CV) measurements were performed with an Autolab PGSTAT 30 potentiostat using a three-electrode set-up with a platinum disc working electrode, a platinum wire was as counter electrode and an $Ag/AgNO_3$ reference electrode and a solution of 0.1 M tetrabutylammonium hexafluorophosphate [NBu_4PF_6] in anhydrous acetonitrile as the supporting electrolyte-solvent system. The reference electrode was calibrated against ferrocene/ferrocenium (Fc/Fc^+) as a standard. The platinum disc working electrode was coated with polymer using a drop casting method from chloroform solution. In order to remove the oxygen from the electrolyte, the system was degassed with Nitrogen before each experiment[1].

The Nitrogen inlet was then moved above the liquid surface and left there during the scan. Cyclic voltammograms were recorded at a scan rate of 100 mVs^{-1}. The HOMO/LUMO energy levels were estimated from the onset potentials of the first oxidation/reduction scans. The HOMO and LUMO energy levels were calculated using **Equations S2** and **S3**, respectively[2]. When the reduction onset potential was not available, the LUMO energy levels were calculated from the values of the HOMO energy levels and the Eg^{opt} using **Equation S4**[1].

$$E_{HOMO} = -(4.4 + E^{OX})eV \quad \text{.....S2}$$

$$E_{LUMO} = -(4.4 + E^{red})eV \quad \text{.....S3}$$

$$E_{LuMO} = -(E_{HOMO} - E^{opt})eV \quad \text{.....S4}$$

1.2.4. X-ray Diffraction

X-ray diffraction (XRD) technique is the most common none destructive technique and efficient method for the determination of structure and crystallinity and material identification. XRD is an apt method to examine whether a resultant material has amorphous or crystalline nature. Crystalline phases can be identified by just comparing the interplanar distance'd' values obtained from XRD data with the fundamental data in Joint Committee on Powder Diffraction Standards (JCPDS).

X-ray diffraction is the elastic scattering of X-ray photons by atoms in a periodic lattice. Copper Kα radiation with the wavelength of 1.540˚A was used as a monochromatic X-ray source to bombard the sample. The scattered monochromatic X-rays that are in phase give constructive interference. The XRD patterns were collected on a Shimadzu diffractometer (XRD - (PANalytical-PW 340/60 X" pert PRO) Measurement Condition X-ray tube operating in the reflection mode with Cu Kα, voltage 40.0 kV, current 30.0 mA radiation at a scanning rate of 4.0000 (deg/min) with 2ϑ ranging from 10^0 to 80^0. Diffraction of X-rays by crystal planes allows one to derive lattice spacing by using Bragg's law **Equation S5**.

$$n\lambda = 2d\sin\theta \quad \text{.....S5}$$

Where, n is an integer called the order of reflection, λ is the wavelength of X-ray, d is the characteristic inter layer spacing between the crystal planes of a given specimen and ϑ is the angle between the incident beam and the normal to the reflecting lattice plane.

1.2.5. Fourier Transform Infrared Spectroscopy

Fourier transform infrared (FT-IR) spectroscopic imaging is a highly versatile, label free and non-destructive chemical imaging method which can be applied to identify unknown materials (unknown compounds), quality or consistency of a sample, and the amount of components in a mixture. FT-IR spectra were recorded on a Shimadzu IR Affinity-1 over a wavenumber range of

4000-1000 cm^{-1} and 4000-600 cm^{-1}. The spectra of samples,Graphite(g), graphite Oxide (GO) and reduced graphene oxide (rGO, pressed into KBr pellets were collected in the wave number range 450 to 4000 cm^{-1} using JASCO FT/IR6200.

1.2.6. Measuring the Charge Carrier Mobility by SCLC

In an organic semiconductor, mobility's are generally much lower than in an inorganic semiconductor, which leads to the build-up of charge. The mobility can be determined experimentally by measuring the current. The measured current is, therefore, space charge limited (SCL). Space charge limited current (SCLC) can be used to determine the mobility of photoactive layer. Considering only one charge carrier (either electrons or holes), the J*SCLC* flowing across a layer with thickness L can be estimated using the Mott-Gurney **Equation S6**[1].

$$J = \frac{9\varepsilon_0\varepsilon_r\mu_h(V)^2}{8L^3} \quad \text{.....S6}$$

Where in J is the current density, *εr* is the relative dielectric permittivity of the organic semiconductor (*εr* = 3), *εo* is the free space dielectric permittivity (8.85×10^{-12} Fm^{-1}), μ_h is the hole mobility, and L is the thickness of the active layer. The effective voltage (V) is related to the applied voltage (V_{apl}) and given by **Equation S7.**

$$V = V_{apl} - V_{bi} \quad \text{.....S7}$$

Wherein the built-in voltage (V*bi*) results from the work function difference between the anode and the cathode (ITO and Al) at which the J–V characteristic becomes quadratic. The hole mobility's can be calculated from the value of the slope of the curve representing the square root of the current density versus the voltage (see **Figure S11**) expressed in **Equation S8**[1, 3].

$$\mu_h = \frac{slpoe^2 8L^3}{9\varepsilon_0\varepsilon_r} \quad \text{.....S8}$$

1.2.7. Atomic Force Microscopy

Atomic Force Microscopy (AFM) is an emerging fundamental tool to deeply investigate morphology. In this regard, AFM measurements were performed under ambient conditions using a Digital Instrument Multimode Nanotec in the tapping mode. The surface of the HTL and active layer films were characterized using a Veeco Dimension 3100 AFM with a Nanotec IV controller and a TESPA-V2 cantilever (37 Nm^{-1} nominal stiffness and 320 kHz nominal resonance frequency) in tapping mode.

1.3. Electrochemical Exfoliation

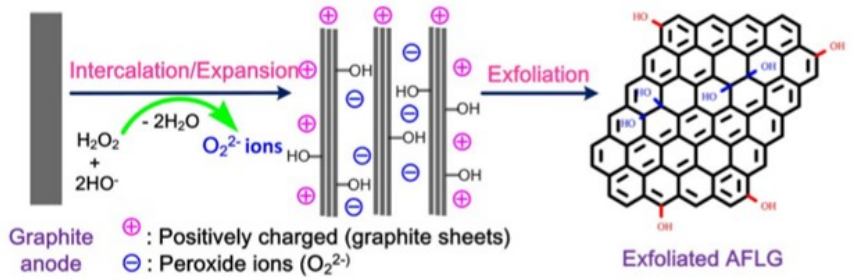

Figure S1. The electrochemical exfoliation mechanism of graphene oxide[4].

1.4. Conductivity Measurements

The conductivity was performed using the digital conductivity meter (Model 4510 Conductivity/TDS Meter). The powder graphite (G), graphene oxide (G), and reduced graphene oxide (rGO) dispersed in deionized water with a concentration variation from 0.004-0.01 ppm. The digital conductivity meter was adjusted by potassium chloride (KCl) solution near 1.395 ms/cm with a cell constant 0.99. Its unit is typically expressed in micro Siemens/cm (µS/cm).

Table S1: The conductivity of G, GO, and rGO in μS/cm.

Con.(ppm)	G	GO	rGO
0.004	9.9	34.7	43.3
0.005	10.3	35	43.6
0.006	10.7	35.8	43.9
0.007	11.4	36.4	44.4
0.008	11.6	37.6	44.6
0.009	11.7	38.3	44.9
0.01	11.8	38.8	45.2

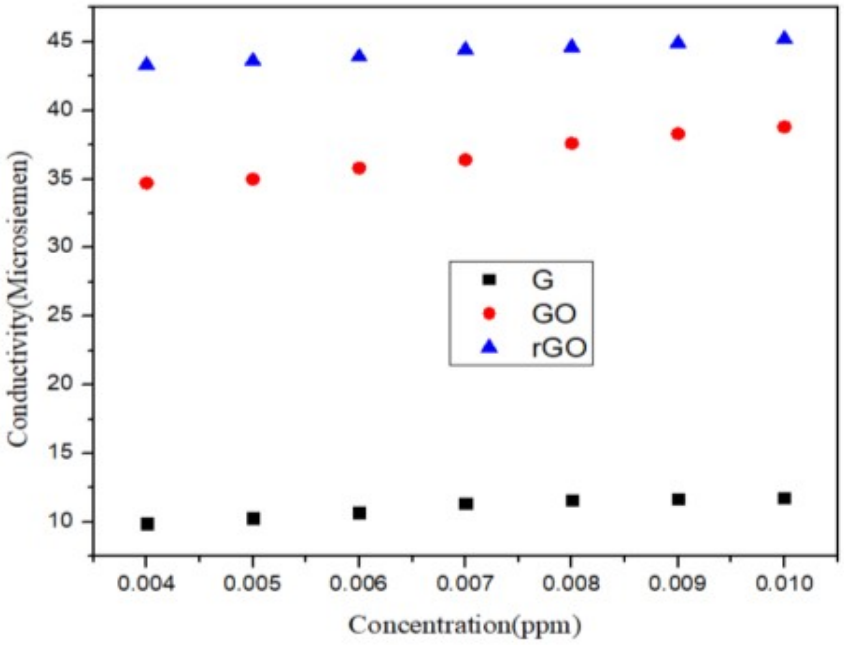

Figure S2. The effects of concentration on conductivity of G, GO, and rGO.

1.5. Optical Properties of Active Layer

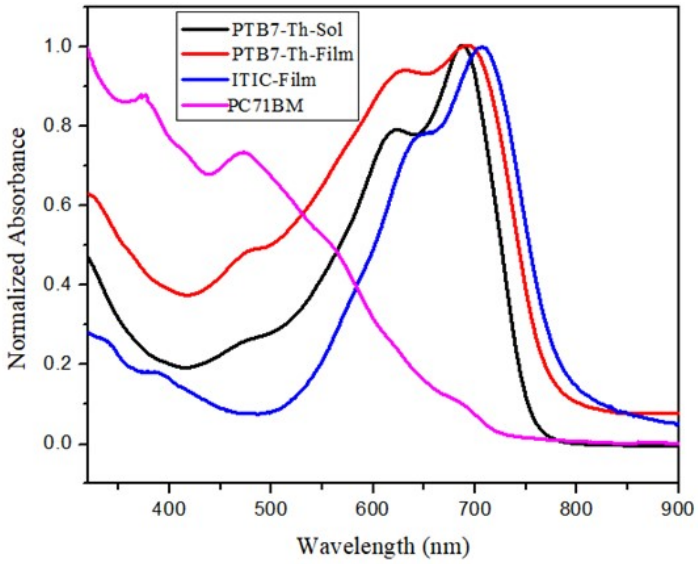

Figure S3. Normalized absorption spectra of PTB7- Th, $PC_{71}BM$, and ITIC in films.

1.6. Electrochemical Properties

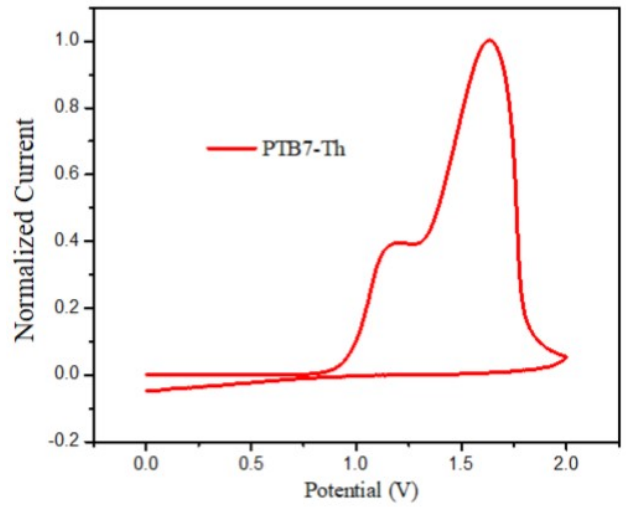

Figure S4. Cyclic voltammograms of the oxidation curves of PTB7-Th.

Figure S4. Normalized absorption spectra of PTB7- Th, PC71BM, and ITIC in films.

1. Electrochemical Properties

Figure S5. Cyclic voltammograms of the oxidation curves of PTB7-Th.

1.7. Device Fabrication and Characterization

1.7.1. Cleaning the Substrates

ITO glass substrates were cleaned using a standard cleaning procedure consisting of a sequence of three ultra-sonication steps in detergent, acetone and isopropanol for 15 minutes each. The samples were dried at ambient conditions. Finally, the glass/ITO-substrates were treated with UV/O_3 for 30 minutes to remove residual organic contaminants from the surface.

1.7.2. PEDOT:PSS, rGO, and PEDOT:PSS:rGO Spin-coating

Aqueous dispersion of rGO was prepared with a rGO/H_2O ratio of 0.25 mg/mL for 90min sonication. PEDOT:PSS (Clevious HTL solar) was filtered through 0.45 µm CA syringe filter. rGO-dispersion was added drop wise to the known volume of filtered PEDOT:PSS until rGO/PEDOT:PSS v/v ratio is 0.2. These dispersions were stirred for 30 min at room temperature. We have employed spin casting to deposit films. These spin-casted films were annealed on hot plate at ~ 130 °C for 15 min[5]. The aqueous PEDOT:PSS dispersion was filtered through a syringe with a 0.45 µm size hydrophilic nylon filter, followed by spin-coating (CHEMAT TECH- NOLOGY SPIN-COATER KW-4A) on top of the cleaned ITO coated substrate at 3500 rpm for 40 seconds to obtain a thickness of ∼ 35-40 nm. The rGO was dissolved in deionized water with a concentration of 1 mg/ml and ultrasoni- cated for 1 hr until a homogeneous solution of rGO was obtained. The rGO solution was spin-coated on the ITO substrates at 4000 rpm for 60 seconds in the atmosphere. Finally, the PEDOT:PSS:rGO composites were prepared by adding rGO/H2O (1mg/ml) drop by drop in to PEDOT:PSS with ratio of 0.05 V/V %. After 1hr of sonication, a homogeneous solution of PEDOT:PSS:rGO was obtained[6]. The PEDOT:PSS:rGO solution was spin coated on the ITO substrates at 4000 rpm for 60 seconds in the atmosphere.

The PEDOT:PSS, rGO, and PEDOT:PSS:rGO coated substrates were then annealed on hot plate at 150 0C for 15 minutes under ambient conditions to remove any residual water. The Glass/ITO/PEDOT:PSS, Glass/ITO/rGO, and Glass/ITO/PEDOT:PSS:rGO-substrates were used for the fabrication of conventional geometry OSCs and hole-only devices.

1.7.3. Solar Cell Device Fabrication

The PTB7-Th:IEICO-4F (1:1.5 wt/wt) blend was dissolved in chlorobenzene (CB) host solvent and 4% CN additive with a total concentration of 15 $mgmL^{-1}$ [7] . The blend solution was stirred overnight (i.e, typically 12 hr) at 50 ^{o}C[8]. Then, on the Glass/ITO/PEDOT:PSS, Glass/ITO/rGO, and Glass/ITO/PED OT:PSS: rGO substrate the photoactive solution PTB7-Th:IEICO-4F were spin-coated at 1000 rpm for 60 seconds. The top electrode, with a thickness of 100 nm was deposited on the top of the active layer through a shadow mask by thermal vacuum evaporator (EDWARDS 306) at a pressure less than 5×10^{-6} mbar to get the device structure as shown in **Figure S6 (a), (b), (c)**, respectively. Silver paste was made at the contact of each electrode just to avoid easy cracking of Al electrode during characterization of the J-V curve. Similarly, the hole only devices were fabricated.

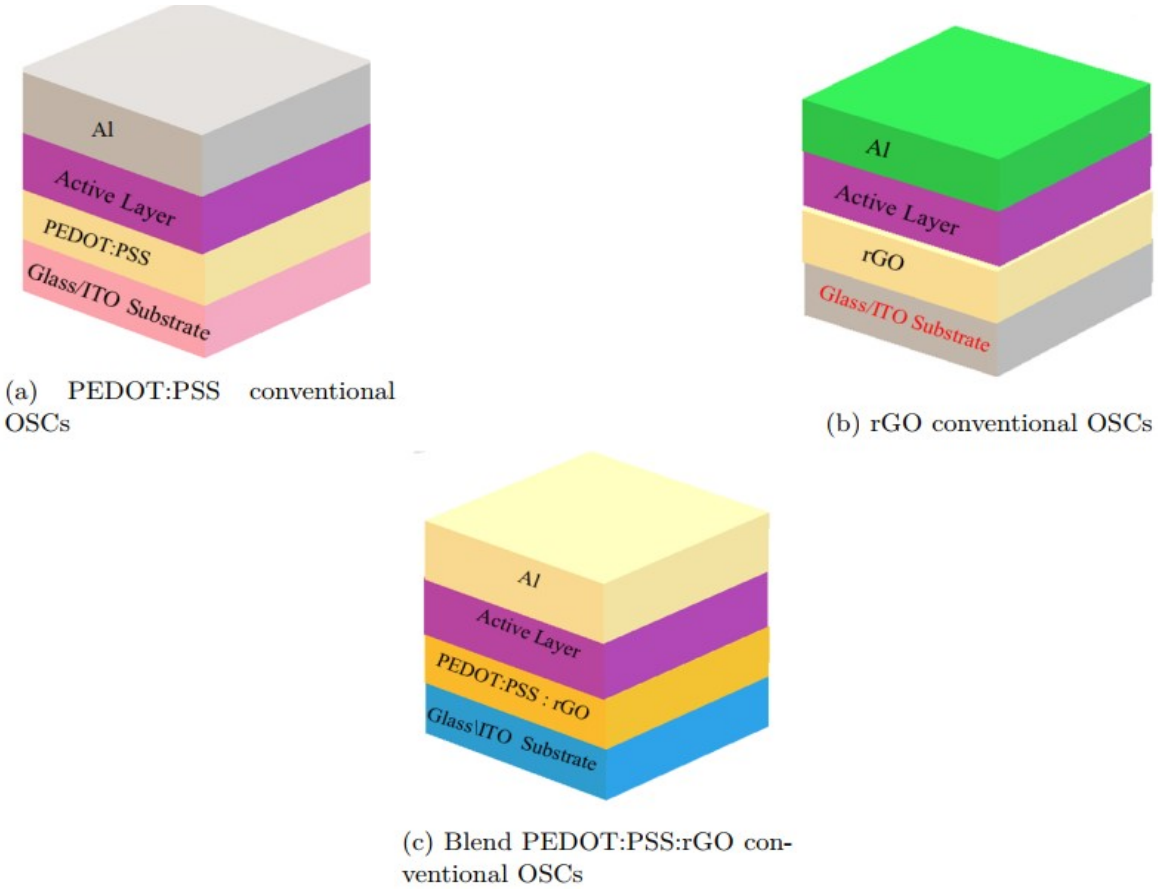

(a) PEDOT:PSS conventional OSCs

(b) rGO conventional OSCs

(c) Blend PEDOT:PSS:rGO conventional OSCs

Figure S5. Device architectures of conventional OSCs with different hole transport layer.

1.8. J-V Curve Measurement

Current density-voltage (J-V) measurements were performed using a computer- controlled potentiostat (CH instrument, Electrochemical Analyzer) in ambient condition under 100 mW cm^{-2} light illuminating using a solar simulator (SS- 50AA Xenon lamp power supply). The J-V curves measurements were recorded by applying a voltage sweep between +1.2 V and -0.2 V. For the hole only devices the J-V curves were recorded by applying a voltage sweep between 0 V to +6 V under dark conditions. The thicknesses of the active layers were determined with a Model: 500 Stylus surface profilometer (KLA Tencor). The film was first scratched by a needle-like toothpick to remove the active layer. Then, the thicknesses of thin films were measured by a Stylus tip in contact with the sample film surface.

1.9. Hole Mobility

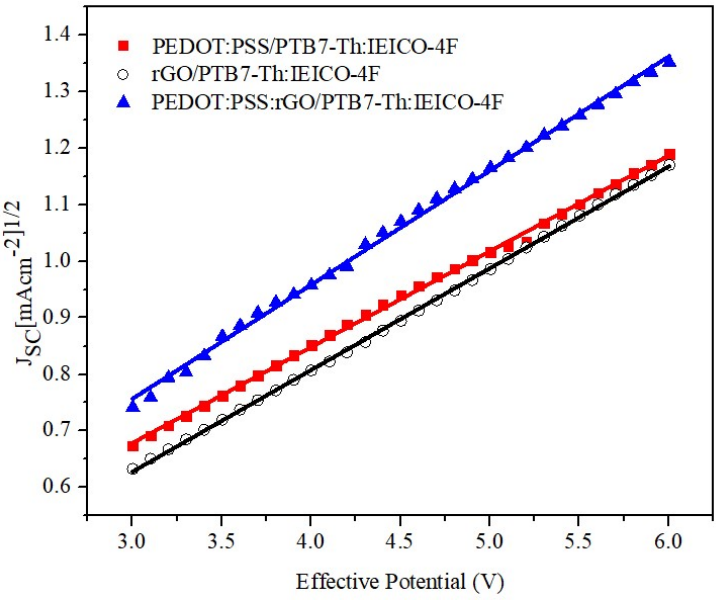

Figure S6. $J^{1/2}$-V curve of hole mobility of PEDOT:PSS/PTB7-Th:IEICO-4F/, rGO/PTB7-Th:IEICO-4F, and PEDOT:PSS:rGO/PTB7-Th:IEICO-4F films.

1.10. Morphological Studies

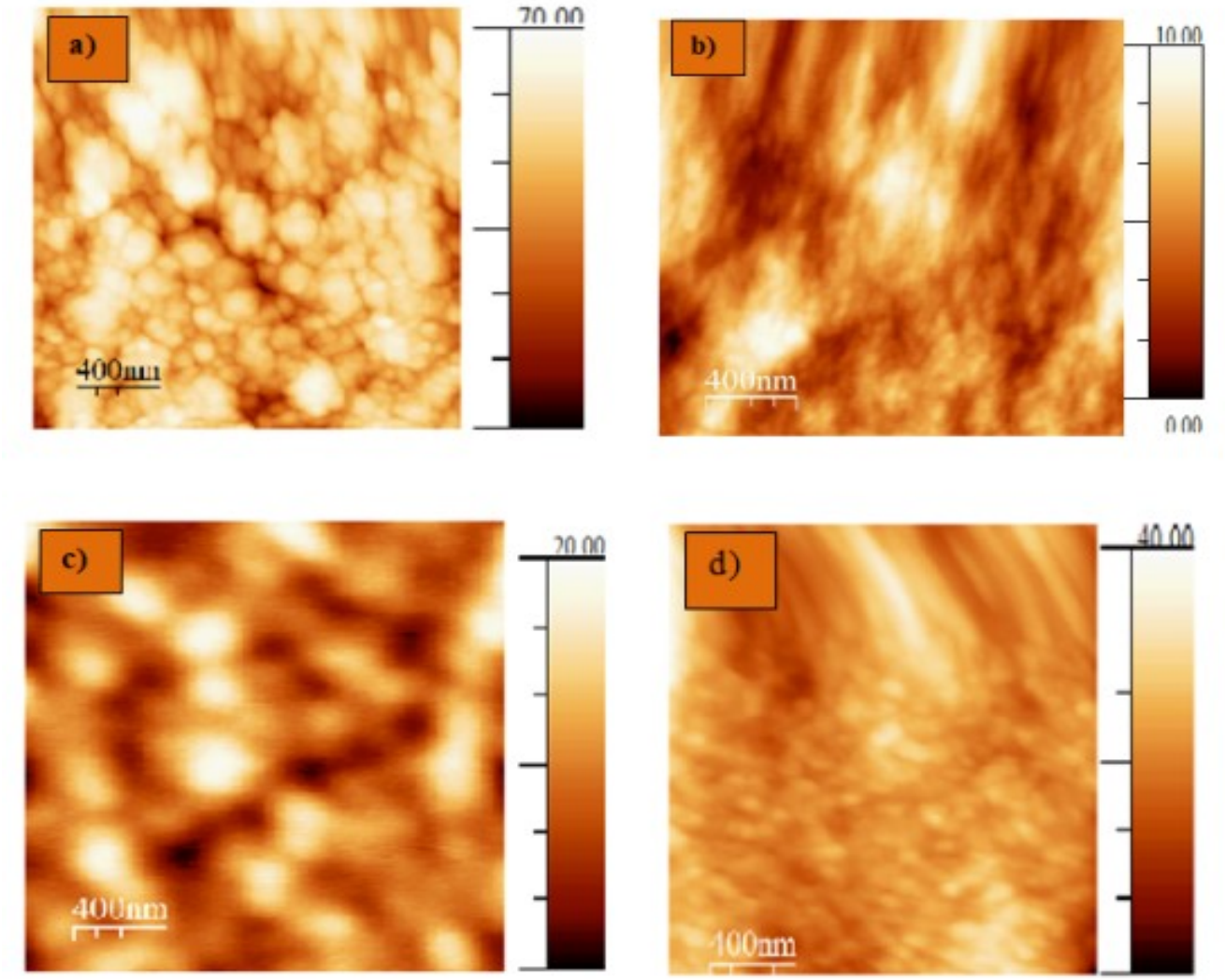

Figure S7. The topography morphology of AFM height images of 2 × 2 μm^2 (a) Glass/ITO film, (b) Glass/ITO/PEDOT:PSS film, (c) Glass/ITO/rGO film, and (d) Glass/ ITO/PEDOT:PSS:rGO film .

References

1. J. Liu, H. Lu, Y. Liu, J. Zhang, C. Li, X. Xu and Z. Bo, *ACS Applied Materials & Interfaces*, 2020, **12**, 10746-10754.
2. V. V. Pavlishchuk and A. W. Addison, *Inorganica Chimica Acta*, 2000, **298**, 97-102.
3. A. Negash, Z. Genene, R. Thiruvallur Eachambadi, J. Kesters, N. Van den Brande, J. D'Haen, H. Penxten, B. A. Abdulahi, E. Wang, K. Vandewal, W. Maes, W. Mammo, J. Manca and S. Admassie, *Journal of Materials Chemistry C*, 2019, **7**, 3375-3384.
4. K. S. Rao, J. Senthilnathan, Y.-F. Liu and M. Yoshimura, *Scientific Reports*, 2014, **4**, 4237.
5. S. Ozcan, M. Erer, S. Vempati, T. Uyar, L. Toppare and A. Cirpan, *Journal of Materials Science: Materials in Electronics*, 2020, **31**, 1-9.
6. D. C. Tiwari, S. K. Dwivedi, P. Dipak and T. Chandel, *AIP Conference Proceedings*, 2018, **1953**, 100065.
7. X. Song, N. Gasparini, L. Ye, H. Yao, J. Hou, H. Ade and D. Baran, *ACS Energy Letters*, 2018, **3**, 669-676.
8. J. Wang, S. Xie, D. Zhang, R. Wang, Z. Zheng, H. Zhou and Y. Zhang, *Journal of Materials Chemistry A*, 2018, **6**, 19934-19940.